NUMERICAL MODELLING OF THE OPERATION OF A TWO-PHASE THERMOSYPHON

by

Veselka KAMBUROVA[a*], Ahmed AHMEDOV[a], Iliya K. ILIEV[a], Ivan BELOEV[a], and Ivan R. PAVLOVIĆ[b]

[a] "Angel Kanchev" University of Ruse, Ruse, Bulgaria
[b] Faculty of Mechanical Engineering, University of Nis, Nis, Serbia

Original scientific paper
https://doi.org/10.2298/TSCI18S5311K

In the recent years, the interest towards the application of two-phase thermosyphons as an element of heat recovery systems has significantly increased. The application of thermosyphons is steadily gaining popularity in a wide range of industries and energy solutions. In the present study, a 2-D numerical modelling of a two-phase gas/liquid flow and the simultaneously ongoing processes of evaporation and condensation in a thermosyphon is presented. The technique volume of fluid was used for the modelling of the interaction between the liquid and gas phases. The operation of a finned tubes thermosyphon was studied at several typical operating modes. A parametric study over a non-ribbed and finned tubes thermosyphon was carried out. The commercial software ANSYS FLUENT 14.0 was used for the numerical analysis. It was proven that the numerical modelling procedure adequately recreates the ongoing flow, heat and mass transfer processes in the thermosyphon. The numerical result from the phase interaction in the thermosyphon was visualized. Otherwise, such visualization is difficult to achieve when only using empirical models or laboratory experiments. In conclusion, it is shown that numerical modelling is a useful tool for studying and better understanding of the phase changes and heat and mass transfer in a thermosyphon operation.

Key words: *CFD dynamics, condensation, evaporation, heat and mass transfer, multiphase flow, two-phase thermosyphon*

Introduction

Heat transfer rate and efficiency are considered as the most important parameters in designing heat exchangers [1]. Thermosyphons are very efficient devices for heat transfer. The closed evaporating multiphase thermosyphon is a vertical or inclined heat pipe filled to about 25-30% with liquid at a pressure lower than atmospheric pressure. The thermosyphon has three separate areas – evaporator area (heating area), adiabatic area (transport area), and condenser area (cooling area). In the evaporator area (the pipe's lower zone) heat is transferred to the working fluid from the flowing over flue gas. The working fluid evaporates and rises to the upper part of the pipe. The vapor condensates on the wall of the pipe over which a cold fluid is flowing (liquid or gas). In the process of condensation, the heat of the vapour is carried out through the pipe walls to the outer cold fluid. The formed condensate travels

* Corresponding author, e-mail: vkambourova@enconservices.com

downwards on the pipe inner walls driven by the force of the gravity. The adiabatic area is located between the evaporation and condensation areas. Regarding the heat exchanger construction, the adiabatic area size may vary significantly, or it can be practically missing.

The heat and mass-transfer processes taking place during a thermosyphon operation are phenomena that needs to be studied in order to gain a deeper insight of the mechanisms that drives them. By using numerical modeling (CFD) in combination with the finite volume method, the aforementioned processes could be simulated. The results of the simulation would yield in temperature fields, volume fraction evaluation and determination of the optimal operating conditions for the investigated heat exchanger.

A lot of researchers have investigated the operation of thermosyphons by the aid of the CFD modeling. In their studies, the researchers have presented results regarding the flow velocity field, the heat and mass transfer processes, and the simultaneous evaporation and condensation phenomena occurring in the two-phase thermosyphons.

Alizadadehdatkel *et al.* [2] used the volume of fluid (VOF) technique to model the multiphase interaction in vertical thermosyphon. Using CFD procedure, they calculated the fluid flow and the temperature fields. They compared the numerical results with experimental data. The numerical modelling showed good agreement with the experimental data.

Annamalai and Ramalingam [3] carried out an experimental and numerical study over a heat pipe. The investigated heat pipe length was 1 m with an outer diameter of 0.03 m. The study was done at two different power inputs at the evaporator section and two different flow rates at the condenser area. The condenser area was cooled by air-flow. The numerical results of the CFD model were compared with the experimental results, the former of which were found to be in reasonable agreement with the latter.

Fadhl *et al.* [4] used CFD approach to model the heat transfer in a two-phase flow during a thermosyphon operation. The authors presented the distribution of two-phase flow and the temperature change during the initial, transient stage of operation and the steady-state operation of a thermosyphon.

Zhang *et al.* [5] developed a 2-D computational model for a two-phase thermosyphon used in electronic cooling. The authors compared the velocity and temperature fields with experimental results in order to determine the main parameters of the thermosyphon. Chaudhari *et al.* [6] presented CFD analysis of a two-phase thermosyphon using the ANSYS-CFX software. The software successfully predicted the overall temperature distribution for the investigated thermosyphon at three different heat inputs. The calculated temperatures at various sections of the thermosyphon were compared with the experimental results.

Lee *et al.* [7] used numerical simulation to analyze the influence of different factors, such as vacuum degree, fill ratio and aspect ratio, on the heat transfer characteristics of a low-watt thermosyphon in natural convection.

Based on the literature review it can be concluded that the smooth walled thermosyphons are investigated in depth. They have undergone a wide range of numerical and experimental investigations carried out by numerous researchers. In contrast with the smooth walled thermosyphon, the finned thermosyphons have not been that intensively researched. The aim of the present study is to compare the temperature and flow fields distributions in a smooth and finned tubes thermosyphon of the same size.

Theoretical formulation

The VOF numerical modeling technique is designed specifically for studying multiphase flow problems. In the case of the VOF numerical procedure, each of the modeled flow

fractions must be defined prior the numerical procedure. The sum of the volume fractions of all the phases in the computational domain (2-D and 3-D) is equal to one. The numerical modelling is carried out simultaneously for all of the flow's phases. The multiphase flow parameters were computed by the following variation of the Navier-Stokes equations [8, 9] in combination with the continuity equation:

– continuity equation

$$\frac{\partial}{\partial t}(\rho)+\sum_{j=1}^{3}\frac{\partial}{\partial x_j}(\rho u_j)=S_{\mathrm{M}} \tag{1}$$

– impulse

$$\frac{\partial}{\partial t}(\rho u_i)+\sum_{j=1}^{3}\frac{\partial}{\partial x_j}(\rho u_i u_j)=-\frac{\partial p}{\partial x_i}+\sum_{j=1}^{3}\frac{\partial}{\partial x_j}\left[\mu\left(\frac{\partial u_i}{\partial x_j}+\frac{\partial u_j}{\partial x_i}-\frac{2}{3}\delta_{ij}\sum_{i=1}^{3}\frac{\partial u_i}{\partial x_i}\right)\right]+S_{F,j} \tag{2}$$

– energy

$$\frac{\partial}{\partial t}(\rho E)+\sum_{j=1}^{3}\frac{\partial}{\partial x_j}(\rho E u_j)=\sum_{i=1}^{3}\sum_{j=1}^{3}\left[\frac{\partial}{\partial x_j}(\tau_{ij})u_i\right]-\sum_{j=1}^{3}\frac{\partial}{\partial x_j}\ q_j+S_{\mathrm{E}} \tag{3}$$

At this variation of the governing equations the density, ρ, and the dynamic viscosity, μ, of the fluid are presented as functions of the volume fractions of each phase, α_κ, and are defined:

$$\rho=\sum_{\kappa=1}^{2}\alpha_\kappa\rho_\kappa \tag{4}$$

$$\mu=\sum_{\kappa=1}^{2}\alpha_\kappa\mu_\kappa \tag{5}$$

The VOF numerical approach for modeling multiphase flows is treating the energy, E, and the temperature, T, as mass-averaged variables. The energy is defined:

$$E=\frac{\sum_{k=1}^{2}\alpha_{\mathrm{k}}\rho_{\mathrm{k}}E_{\mathrm{k}}}{\sum_{k=1}^{2}\alpha_{\mathrm{k}}\rho_{\mathrm{k}}} \tag{6}$$

where E_{k} for each phase depends on the interaction of the specific heat and the temperature fields of the individual phases. The continuity of α is carried through an interface mass balance, depicted by the following equation:

$$\frac{\partial\alpha}{\partial t}+u\nabla\alpha=0 \tag{7}$$

When $\alpha = 1$, the whole volume of the computational domain is occupied by the gas phase. In the case when $\alpha = 0$, the whole volume is occupied by the liquid phase. The interface (contact) regions between the two phases were formed in the areas where $\alpha = 0$-1.

When the temperature of the liquid phase exceeds the saturation temperature T_{sat}, a component with mass rate of S_M transfers from liquid phase to vapor phase, during which a certain amount of energy E is absorbed.

Experimental equipment, model geometry and computational mesh

For the current study, the commercial CFD software ANSYS FLUENT 14.0 was used. The VOF technique was adopted for modeling the operation of a closed thermosyphon. The thermosyphon's operational regimes were characterized by phase changes occurring in their work fluid (most likely water). The liquid in the evaporator zone was heated over the saturation temperature, which results in evaporation. The vapor travels to the condenser area, it cools down and forms a condensate layer on the thermosyphon's walls. The condensed liquid flows down to the evaporator area and the process repeats itself.

The main goal of this paper is the development of a 2-D computational model in order to study the two-phase flow and the heat transfer during a thermosyphon operation.

The subject of the present study is closed thermosyphons with smooth and finned walls. The thermosyphon was made from Cu with wall thickness of 2 mm and total length of 928 mm. The 3-D models of the investigated thermosyphons are shown in fig. 1. In the two variations of the thermosyphons (smooth and finned tubes) the length of the evaporator area was 680 mm, the condenser area has length of 246 mm. The outer and inner diameters of the thermosyphon were: 24 mm and 20 mm. The diameters of the tubes in the finned tubes thermosyphon was 60 mm with thickness of 2 mm. The total number of fins was 10. This was done in order to keep the number of computational cells in reasonable limits.

Figure 1. The 3-D models of the studied thermosyphons; (a) thermosiphon with smooth walls, (b) thermosyphon with finned tubes

The geometry and the computational mesh were created by the Design Modeler and MESH computer software, which are available in the ANSYS 14.0 software package. In the geometrical model two separate zones were established, one for the wall and one for the fluid domain. The computational mesh for the variation of the thermosyphon with smooth walls consists of about 89472 cells. While the ribbed variation consists of about 94320 cells. The sectional area of the smooth thermosyphon was 0.022368 m^2, while the sectional area of the finned tubes thermosyphon was 0.23568 m^2. The implemented computational mesh was structural, quadrilateral. The height of the first cell row near the walls was 0.01 mm. The used growth rate factor was 1.2. The generated computational mesh for both the smooth and finned tubes thermosyphons was shown in fig. 2. During the development of the 2-D geometrical model of the finned tubes thermosyphon the number of the fins was significantly reduced in comparison to the referenced finned tubes thermosyphon. This simplification was made in order to keep the number of computational cells in reasonable limits.

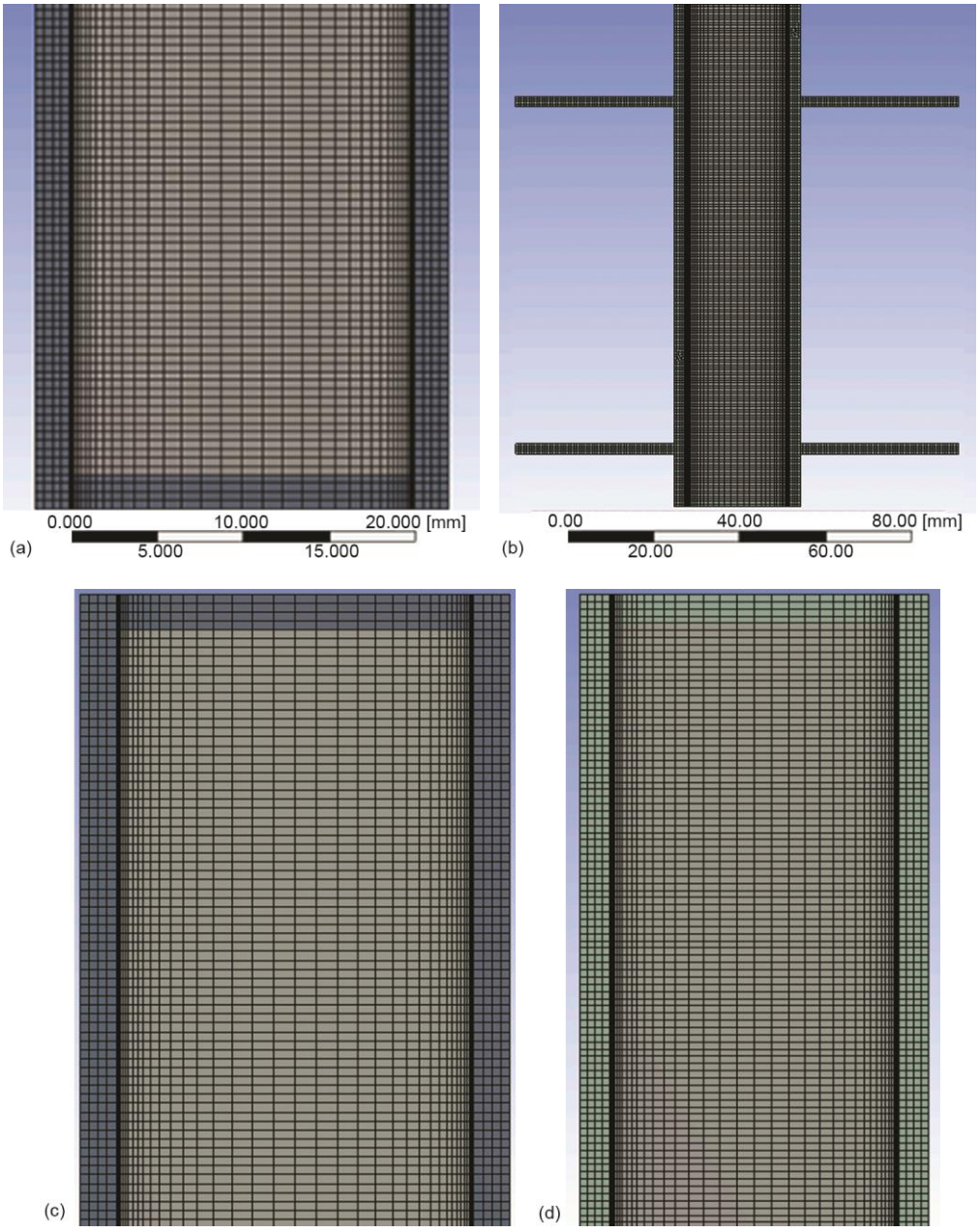

Figure 2. Generated computational mesh of the smooth and finned tubes thermosyphon; (a) computational mesh in the evaporator area – smooth thermosyphon, (b) computational mesh in the area of the evaporator – finned tubes thermosyphon, (c) computational mesh in the condenser area – smooth thermosyphon, (d) computational mesh in the condenser area – finned tubes thermosyphon

The accuracy of the numerical solution depends on the correct modeling of the laminar sublayer in the near-wall region. Due to that reason, the applied mesh in the near-wall region is structural, quadrilateral and refined. The near-wall criteria y^+ value gives an overall

evaluation over the near-wall mesh quality, and the adequate operation of the numerical procedure. This dimensionless parameter characterizes the distance from the wall to the node of the first cell element. The near-wall criteria is given by:

$$y^+ = \frac{\rho U_\tau y}{\mu} \tag{8}$$

where ρ is the water density, y – the normal distance from the wall to the first computational node, $U_\tau = (\tau_\omega/\rho)^{1/2}$ – the frictional velocity, $\tau_\omega = \mu(\partial u/\partial y)$ – the near-wall share stress, defined by the velocity gradient in normal direction, and μ – the water dynamic viscosity.

The accuracy of the numerical modelling is determined by the y^+ value:

– the range $30 < y^+ < 300$ is appropriate for numerical procedures with wall function turned on. In these cases, the mesh density in the near-wall region allows for the modeling of the flow only to the turbulent region of the laminar sublayer $y^+ > 30$ and
– the range $1 < y^+ < 5$ is appropriate for numerical procedures that account for the modeling of the entire laminar sublayer. In these cases, the mesh density in the near-wall region is sufficient to allow adequate laminar sublayer modeling.

In the present study, the mesh properties applied in the near-wall region results in $y^+ \leq 5$. This value of the near-wall criteria guarantees acceptable modeling of the laminar sublayer.

Boundary conditions

A constant heat flux boundary condition was applied to the walls in the evaporator area. The heat flux value was 300 W/m^2. For the adiabatic area, a zero-heat flux boundary condition was applied to the walls. In the condenser area, a convective heat transfer boundary condition was specified. The convective heat transfer was defined by assigning a convective heat transfer coefficient to the walls with value of 180 W/(m^{2}K). In the contact region of the walls and the fluid domain a coupled walls interface boundary condition was applied. The pressure for the operating condition in the thermosyphon was set to 30 kPa. The corresponding saturation temperature for this pressure was 69.1 ºC. A gravitational constant of 9.81 m/s^2 was set. The used boundary conditions are presented in fig. 3.

The flow regime in the thermosyphon was determined by the Reynolds criteria. The value of the Reynolds criteria is given by:

$$\mathrm{Re} = \frac{\rho \upsilon D}{\mu} \tag{9}$$

where $\rho = 1000$ [kgm^{-3}] is the water density, $D = 0.02$ [m] – the thermosyphon inner diameter, and $\mu = 8.9 \cdot 10^{-4}$ [Pa·s] – the water dynamic viscosity.

In a preliminary steady-state numerical modeling of the thermosyphon flow it was determined that the average flow velocity was $\upsilon = 0.1$ m/s.

Taking into account these values the Reynolds criteria is calculated as Re = 2.247. As the criteria value is $\mathrm{Re} \leq 2.320$, therefore the flow regime is laminar.

Numerical procedure

An unsteady analysis over the operation of the two variations of the thermosyphon was carried out. The unsteady analysis allows for the adequate modeling of the vigorous multiphase flow processes taking place during the thermosyphon operation. The time step size was set to 0.00005 secons. The time step size was chosen in regard of the Courant-Friedrichs--Lewy (CFL) number. At the current time step size, the average CFL number was under 1.6.

The maximum CFL number for VOF simulation was 250. Due to limitations regarding the computational hardware and the computational time, the modeled operation time for both variations of the thermosyphon was limited to 1 second.

The CFD software FLUENT 14.0 offers a wide range of segregate computational schemes for pressure-velocity coupling. In order to reduce the computational time and avoid solution divergence the following settings were used – SIMPLE segregate solver for the pressure-velocity coupling, first order upstream scheme for the energy and the momentum. For the spatial discretization of the individual fractions, the geo-reconstruction algorithm was used. For the pressure calculation, the PRESTO scheme was chosen. In the present study, the values for the scaled residuals at which the solution converges were set to 10^{-4} for the mass and velocity components and 10^{-6} for the energy. In order to reduce the overall size of the acquired data from the solution the solver was set to save the data at every 500-time steps. The number of iterations per time step was set to 300.

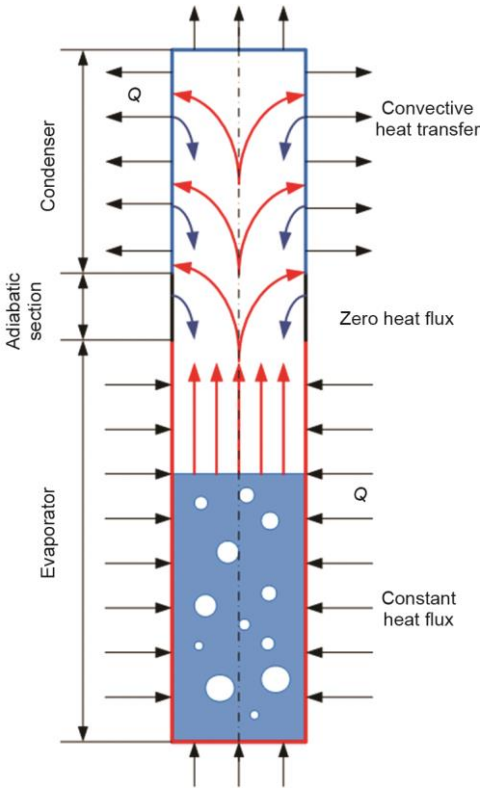

Figure 3. Boundary conditions applied to the thermosyphon model

The vapor phase of the working fluid was set as primary, while the liquid phase was set as secondary. The tertiary phase was assigned to the air volume fraction. The air fraction was added in order to initially fill the empty space over the liquid phase which will allow for accurate unsteady modeling of the evaporation process.

Computational hardware parameters

The computational hardware used for this 2-D modeling were as follow: CPU, 2 pcs. – Intel Xenon CPU E7-4820 2 GHz with a total number of cores 32 of which FLUENT 14.0 uses 20 cores due to license limitations, RAM 128 GB, GPU – NVIDIA Quadro 4000, HDD – 1,6 TB. Each of the 20 VOF simulations took about 26-28 hours. The time needed to set up the modeling procedure and the time needed to extract the results from the numerical solution were not taken into account.

Results and discussions

The results obtained by the CFD simulation regarding the distribution of the liquid and vapor phases during the operation of the smooth and finned tubes thermosyphons are presented in fig. 4. The presented data depicts the initial vaporization process which starts at the evaporator area of the thermosyphon. It can be seen that the formed vapor bubbles travel from the evaporator area towards the condenser area. At the time of 30 seconds the vapor bubbles have not reached the top end of the condenser area in the case of the smooth thermosyphon. But after 60 seconds the vapor bubbles take almost the whole volume of the thermosyphon.

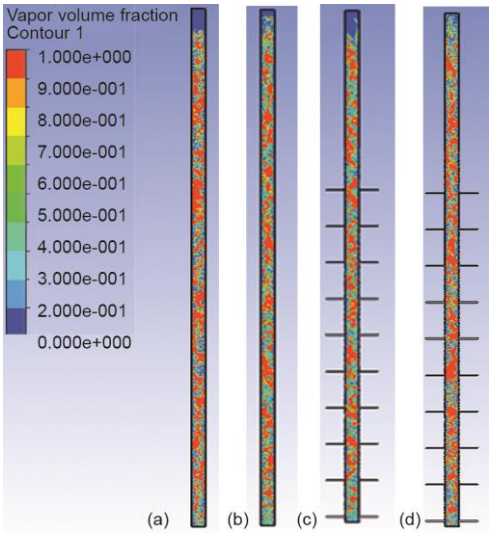

Figure 4. Volume fraction contours of the boiling process in the thermosyphon; (a) smooth pipe, t = 30 s, (b) smooth pipe, t = 60 s, (c) ribbed pipe, t = 30 s, (d) ribbed pipe, t = 60 s (*for color image see journal web site*)

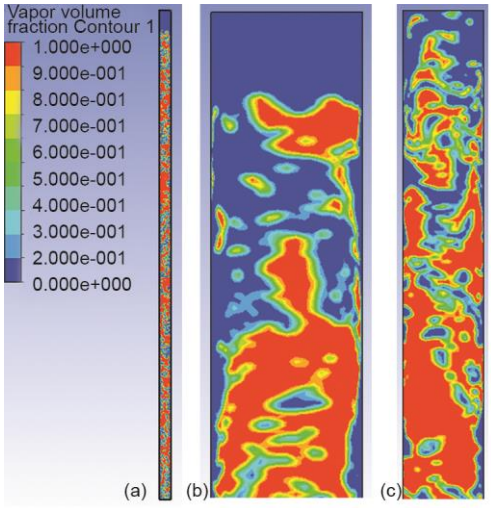

Figure 5. Volume fraction contours at the condenser area for the case of smooth and ribbed thermosyphon of time 60 seconds (*for color image see journal web site*)

In the case of the finned tubes thermosyphon, at time 1 minute the vapor bubbles were filling a significant portion of it. In this case it can be noted that the volume filled with vapor bubbles was significantly larger in comparison with the smooth thermosyphon. This was due to the larger heating area of the finned tubes thermosyphon.

During the operation of the thermosyphon the liquid phase diminishes while the vapor phase grows. The saturated steam formed in the evaporator area travels through the adiabatic area and finally reaches the condenser area. As a result of the thermosyphon's outer wall cooling in the condenser area by the external fluid-flow, the wall temperature was lower than the vapor saturation temperature. This triggers the condensation process of the vapor phase over the walls in the condenser area of the thermosyphon. This process is depicted in fig. 5. As can be seen from the figure a liquid film starts to form in the near wall region at the condenser area. In the case of the finned tubes thermosyphon the vapor phase takes a larger portion of the condenser area volume in comparison with the smooth thermosyphon. At time 60 seconds the vapor phase was the dominant one through the whole volume of the thermosyphon.

Temperature distribution

The temperature distribution fields for the cases of smooth and finned thermosyphon are shown in fig. 6. Comparison of the temperature fields of smooth and finned thermosyphon shows that the temperature in the vaporizer of the finned thermosyphon is higher than that of the smooth one by (5-6) °C. This is due to the larger heat exchange surface of the finned thermosyphon, where the resulting vapors are heated to a higher temperature. In the case of the smooth thermosyphon, the lowest temperature was observed at the top end of the condenser where the cooling process has begun. The same situation was observed in the finned tubes thermosyphon. Over time, the temperature in the cooling part increases. In all of the studied cases, it is clearly observed that the temperature near the wall is lower than that at the center of the flow due to the heat exchange process and the condensation of the vapor. The temperature field distribution has not reached a quasi-steady state, which would require modelling a

larger time span of the thermosyphon's operational time. Thus, more precise result analysis can be obtained.

Experimental results

The experiment was carried out on a set consisting of a thermosyphon, a heater and a cooler, fig. 7. The thermosyphon was made from Cu with wall thickness of 2 mm, total length of 928 mm, the length of the evaporator area was 680 mm, and the condenser area has length of 246 mm. The outer and inner diameters of the thermosyphon were: 24 mm and 20 mm. The thermosyphon is finned in the evaporation zone (1), with the number of ribs amounting to 10. The pressure for the operating condition in the thermosyphon was set to 30 kPa. The thermosyphon was filled with distilled water, the fill rate being ε = 30%.

The thermosyphon is positioned vertically. Heat is fed to the evaporation zone by means of an electric heater – 2, fig. 7, connected to a laboratory transformer – 4. The magnitude of the heat flow is controlled by the wattmeter – 3. The surface temperature of the thermosyphon was measured by ten Cu constantan thermocouples equally spaced along the thermosyphon. All thermocouples used for the measurements are calibrated and a maximum uncertainty of ±0.1 °C was found. These thermocouples are connected to a data acquisition system. The thermocouple locations are shown in fig. 8. Heat removal from the top of the thermosyphon was done by means of a heat exchanger tube in tube – 5, fig. 8. The water consumption was measured by a rotameter and the temperature of the inlet and outlet of the heat exchanger with nine Cu constantan thermocouples. According to the flow, temperature and heat balance measurements of the heat exchanger, the heat flow from the heat sink to the cooling water was calculated and the convective heat transfer coefficient was calculated at 180 W/m^{2}K.

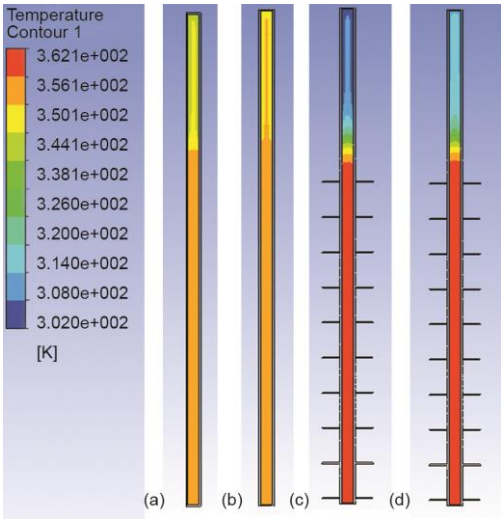

Figure 6. Temperature distribution for smooth and finned tubes thermosyphons; (a) smooth pipe, *t* = 30 s, (b) smooth pipe, *t* = 60 s, (c) ribbed pipe, *t* = 30 s, (d) ribbed pipe, *t* = 60 s
(*for color image see journal web site*)

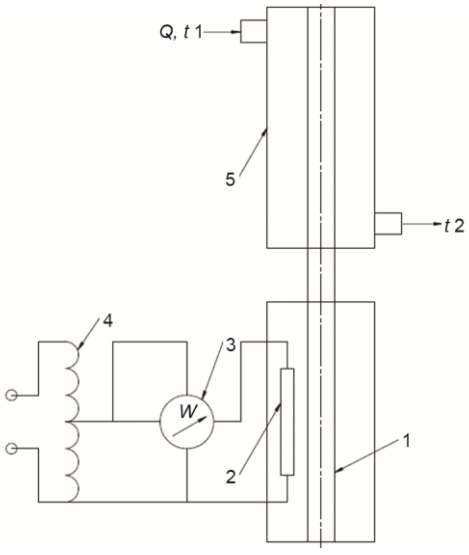

Figure 7. Scheme of the experimental setting

Comparison between calculated and experimental temperatures

In the experimental study, the temperature of the ribbed thermosyphon was measured at ten different points. Considering the high heat conductivity coefficient of Cu, it can be assumed that this is the temperature of the fluid in the near wall layer.

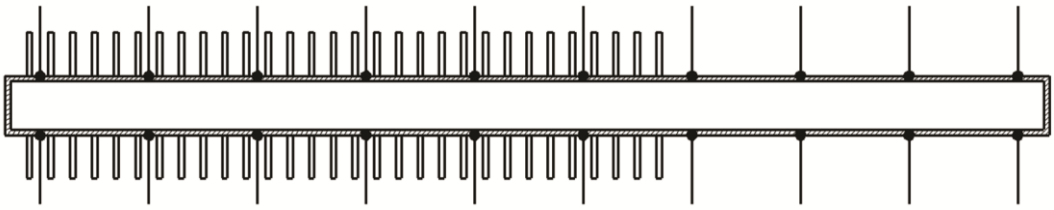

Figure 8. Thermosyphon thermocouple location

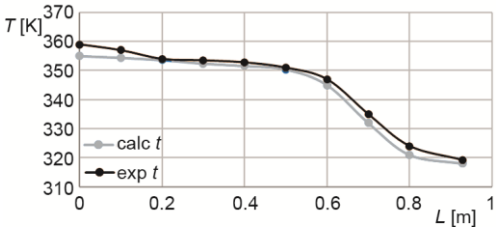

Figure 9. Comparison of the surface temperature of the CFD and experimental results

Figure 9 shows the calculated and experimental result of the surface temperature distribution along the length of the pipe. The axial distance between 0-0.6 m is the evaporator zone and between 0.7-1.0 m is the condenser zone. It is seen from the figure that during the initial period of approximately 60 seconds, there is a continuous decrease in the temperature along the length of the thermosyphon. The comparison between the calculated and the experimental results shows that the largest deviation between them is in the evaporation region (L = 0 m) and is equal to 4 K.

Conclusions

The application of the thermosyphons is gaining popularity in heat utilization from flue gas. In this paper, a CFD approach was used to model the operation of a smooth and finned tubes thermosyphons. The developed method allows for the simulation of the two-phase flow and heat transfer taking place during the thermosyphon operation.

The thermosyphon was filled with distilled water. The heat distribution fields for the two variations of the thermosyphon were obtained. The two-phase flow field for the two variations are visualized.

The commercial CFD software ANSYS FLUENT 14.0 was used in the present study. The specialized software package allowed for the modelling of the complex two-phase flow and heat and mass-transfer processes taking place during the smooth and finned tubes thermosyphons operation.

The results of an experiment carried out under the conditions adopted in developing the model are presented. The comparison of the calculated and experimental results shows good coincidence.

This study proves that the developed 2-D CFD approach is able to simulate the complex flow and thermodynamics processes taking place during the smooth and finned tubes thermosyphon operation. The numerical procedure takes into account all of the simulations processes of heat transfer, evaporation, condensation and the phase changes from liquid to vapor and vice versa.

Nomenclature

D – thermosyphon inner diameter, [m]
E – energy, [J]
S_M – mass source term
$S_{F,j}$ – impuls source term
S_E – energy source term
q – heat flux density, [Wm^{-2}]

T – temperature, [K]
U_τ – the frictional velocity, [ms^{-1}]

Greek symbols

α_κ – volume fractions of each phase, [–]
μ – dynamic viscosity of the fluid, [Pa·s]
ρ – density of the liquid phase of the fluid, [kgm^{-3}]
τ_ω – the near-wall share stress, [Pa]

Subscripts

k – volume fraction (liquid/vapour)
sat – saturation temperature

References

[1] Ghazanfari, S. A., Wahid, M. A., Heat Transfer Enhancement and Pressure Drop for Fin-and-Tube Compact Heat Exchangers with Delta Winglet-Type Vortex Generators, *Facta Universitatis – Series Mechanical Engineering*, *16* (2017), 2, pp. 233-240
[2] Alizadehdakhel, A., *et al.*, CFD Modeling of Flow and Heat Transfer in a Thermosyphon, *International Communication in Heat and Mass Transfer*, *37* (2010), 3, pp. 312-318
[3] Annamalai, A. S., Ramalingam, V., Experimental Investigation and Computational Fluid Dynamics Analysis of an Air Cooled Condenser Heat Pipe, *Thermal Science*, *15* (2011), 3, pp. 759-772
[4] Fadhl, B., *et al.*, Numerical Modelling of the Temperature Distribution in a Two-Phase Closed Thermosyphon, *Applied Thermal Engineering*, *60* (2013), 1-2, pp. 122-131
[5] Zhang, M., *et al.*, Numerical Simulation and Experimental Verification of a Flat Two-Phase Thermosyphon, *Energy Conversion and Management*, *50* (2009), 4, pp. 1095-1100
[6] Chaudhari, N. E., *et al.*, Computational Fluid Dynamics Analysis of Two-Phase Thermosyphon, *International Journal of Engineering and Technology (IJET)*, *5* (2013), Oct.-Nov., pp. 3794-3800
[7] Lee, C.-Y., *et al.*, Numerical Simulation of the Heat Transfer Characteristics of Low-Watt Thermosyphon Influence Factors, *Journal of Applied Science and Engineering*, *17* (2014), 4, pp. 423-428
[8] Hirt, C., Nichols, W, B. D., Volume of Fluid (VOF) Method for the Dynamics of Free Boundaries, *Journal of Computational Physics*, *39* (1981), 1, pp. 201-225
[9] ***, ANSYS Fluent 14.0, Fluent Theory Guide

Paper submitted: March 6, 2018
Paper revised: October 6, 2018
Paper accepted: October 9, 2018